Multiple broken symmetries in striped $La_{2-x}Ba_xCuO_4$ detected by the field-symmetric Nernst effect

Anjan Soumyanarayanan,[1,2,*] X. Y. Tee,[1] T. Ito,[3] T. Ushiyama,[3] Y. Tomioka,[3] and C. Panagopoulos[1,†]

[1]*Division of Physics and Applied Physics, School of Physical and Mathematical Sciences, Nanyang Technological University, 637371 Singapore*

[2]*Data Storage Institute, 5 Engineering Drive 1, 117608 Singapore*

[3]*National Institute of Advanced Industrial Science and Technology, Tsukuba, Ibaraki 305-8562, Japan*

(Received 18 June 2015; revised manuscript received 24 October 2015; published 11 February 2016)

We report a thermoelectric investigation of the stripe and superconducting phases of the cuprate $La_{2-x}Ba_xCuO_4$ near $x = 1/8$. We vary the doping and the magnetic field to identify features in the field-symmetric Nernst effect consistent with the reports of time-reversal symmetry breaking above the superconducting T_c. Crucially, we further detect a field-invariant peak at the stripe charge order temperature, T_{CO}. Our observations suggest the onset of a nontrivial charge ordered phase at T_{CO}, and the subsequent presence of spontaneously generated vortices before the emergence of bulk superconductivity.

DOI: 10.1103/PhysRevB.93.054512

I. INTRODUCTION

There is increasing evidence of a fundamental connection between the phenomenology of unconventional superconductivity and the proliferation of broken-symmetry phases in hole-doped cuprates [1–3]. On one hand, numerous studies indicate the existence of electronic phases that break translational symmetry, viz. spin/charge density waves [4,5] and stripes [6], and are expected to compete with or enhance superconductivity. On the other hand, several reports of the onset of broken time-reversal and point-group symmetries have recently emerged [7,8], complicating the picture. A case in point is the prototypical cuprate $La_{2-x}Ba_xCuO_4$, wherein the doped holes form a $\sim 8a_0$-periodic spin stripe arrangement [6,9]—strongest at $x = 1/8$—where bulk superconductivity is strongly suppressed [10]. Recent reports suggest that striped LBCO may also host other broken symmetries, with potential ramifications on the extensively debated superconducting mechanism in these materials [11–14].

A set of recent studies on 1/8-LBCO have challenged the notion that its phase diagram is well understood. First, a recent transport study by Li *et al.* [11] has detected a finite Nernst effect signal *at zero magnetic field* well above T_c, interpreted as evidence of spontaneous vortex generation due to time-reversal symmetry breaking (TRSB). This was corroborated by the polar Kerr effect measurements of Karapetyan *et al.* [12]. However, subsequent theoretical work showed that these observations could also be consistent with a nontrivial point-group symmetry breaking (PSB) induced by stripe charge order [13,14], wherein the stacking of stripes in the *a*-*b* plane can be modulated in a nontrivial fashion along the *c* axis to break inversion and mirror symmetries. It is worth noting that the onset of stripe order plays a central role in both scenarios—the TRSB is driven by the onset of superconducting correlations along individual stripes, whereas the PSB is ascribed to the spatial ordering of stripes. Several prior observations such as that of a pairing gap and resistivity drop above T_c [15–18] support the presence of superconducting correlations, corroborating the TRSB picture. Meanwhile, some predictions ensuing from PSB dealing with the variation of the Kerr angle with the crystal orientation have also been verified [13]; however, this interpretation remains a subject of controversy [2,19–22]. Importantly, neither scenario provides a fully satisfactory explanation of recent experiments—the sign of the TRSB signal cannot be "trained" by external magnetic fields, while PSB cannot explain the Nernst effect profile, observed to peak near the onset of superconductivity [11].

Here, we perform a high-resolution thermoelectric investigation of near-1/8 LBCO, and use the doping and field dependence of the observed features to delineate their behavior and understand their origin. Our high-resolution Nernst effect measurements show TRSB signatures consistent with prior reports [11], and further detect a sharp, field independent peak at the stripe charge ordering temperature T_{CO}. Our observations suggest the onset of a nontrivial stripe charge ordered phase at T_{CO}, and the subsequent presence of spontaneously generated vortices over a broad temperature range before the onset of bulk superconductivity in LBCO.

II. METHODS AND RESULTS

Single crystals of $La_{2-x}Ba_xCuO_4$ (near $x = 1/8$) were grown using the laser-diode-heated floating zone method, which enables an exceptionally high degree of sample homogeneity [23]. The samples were cut along the crystal axes into rectangular bars for *a*-*b* plane transport measurements. For thermoelectric measurements, the typical temperature gradient applied was $\nabla T \sim 0.1$ K/mm. The accuracy and reproducibility of the field-symmetric Nernst effect results were ensured by measuring the Nernst and Seebeck coefficients simultaneously [Fig. 2(a)]. Further experimental methods are detailed in Ref. [24].

The phase diagram of hole-doped LBCO ($x \sim 0.1$–0.2) has been extensively characterized by a combination of scattering, transport and thermodynamic measurements, establishing the signatures of stripe and superconducting transitions in such measurements [10,11,17,25,26]. Our measurements of in-plane resistivity [ρ_{ab}, Figs. 1(b) and 1(c)] and out-of-plane magnetization [M, $H \parallel c$, Figs. 1(d) and 1(e)] show the series

*anjans@ntu.edu.sg
†christos@ntu.edu.sg

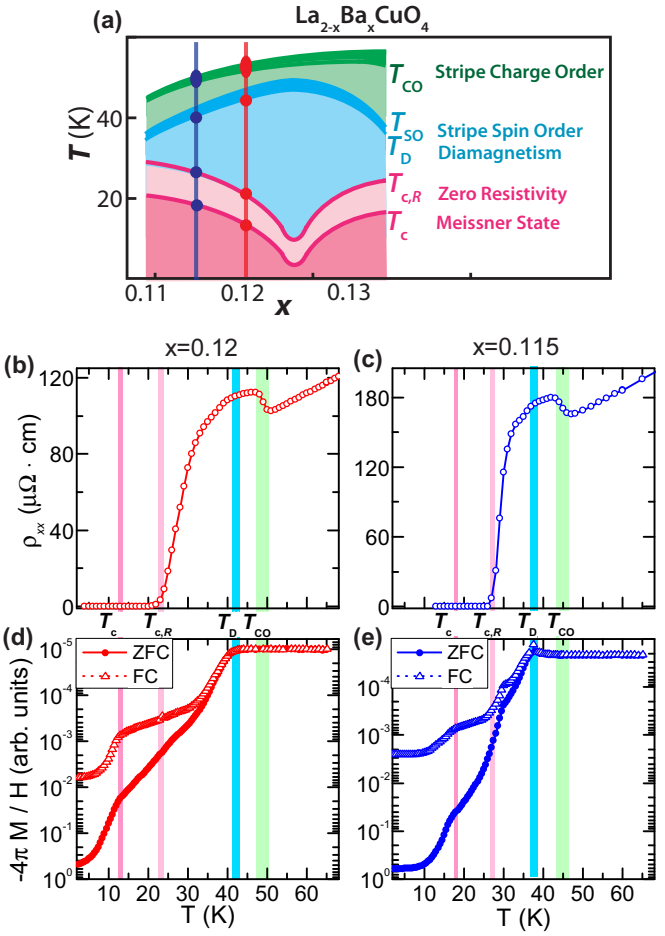

FIG. 1. Resistivity and magnetization. (a) Schematic phase diagram of $La_{2-x}Ba_xCuO_4$ around $x = 1/8$, with characteristic temperatures of stripe and superconducting phases indicated. The relevant doping for samples studied in the work are shown in red ($x = 0.12$) and blue ($x = 0.115$), respectively, with closed circles indicating observed transitions [24]. [(b) and (c)] In-plane resistivity (ρ_{ab}) and [(d) and (e)] magnetization ($H \parallel c$) for representative samples with $x = 0.12$ [(b) and (d)] and $x = 0.115$ [(c) and (e)], respectively. Temperatures corresponding to stripe and superconducting transitions are identified using vertical lines, and correspond to kinks in the resistivity and magnetization curves.

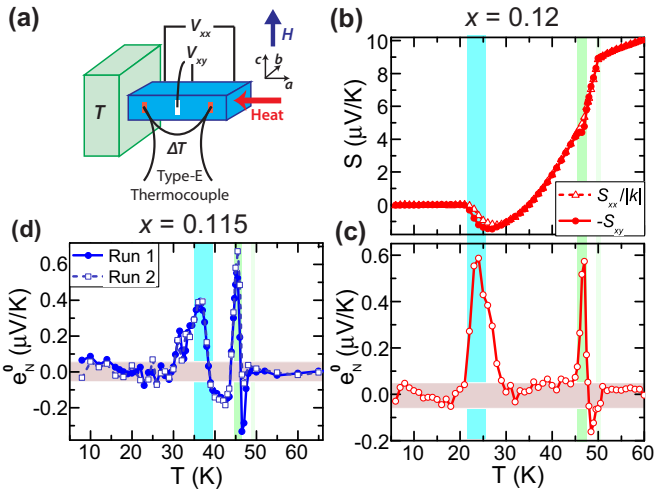

FIG. 2. Zero-field Nernst effect. (a) Schematic contact configurations for simultaneous Seebeck (longitudinal, or S_{xx}) and Nernst (transverse, or S_{xy}) effect measurements. Inset shows the crystalline axes orientation for the samples. (b) The measured zero-field Seebeck ($S_{xx}/|k|$, $k = -4.5$) and Nernst (S_{xy}) coefficients for $x = 0.12$ as a function of temperature, overlaid by superposing their values above 55 K [11]. (c) True zero-field Nernst (ZFN) signal, $e_N^0(T)$ for $x = 0.12$ extracted by subtracting the longitudinal pickup [$S_{xx}(T)$] from the measured Nernst response [$S_{xy}(T)$] using (b). Finite contributions to $e_N^0(T)$ are observed just above $T_{c,R}$ and at T_{CO}. (d) Similarly obtained ZFN signal $e_N^0(T)$ for $x = 0.115$, showing features consistent with (c), recorded across two runs, with fresh electrical contacts and thermocouples used for each run.

of transitions that our LBCO samples undergo when cooled below 80 K [schematic Fig. 1(a)]: (1) onset of $\sim 4a_0$ periodic charge order at T_{CO} (45–48 K), triggered by the formation of a low-temperature tetragonal (LTT) structural phase; (2) onset of $\sim 8a_0$ periodic spin order at T_{SO} ($\sim 40 - 42$ K, not detectable); (3) onset of diamagnetism at T_D ($\sim 38 - 40$ K); (4) zero resistivity at $T_{c,R}$ ($\sim$ 21–26 K); and (5) emergence of 3D superconductivity below T_c (12–18 K). Further details of the identification are discussed in Ref. [24]. We emphasize the quantitative consistency of these temperature scales within our experiments [24] and note their agreement with existing literature [10,17,18].

To distinguish the evidence for TRSB due to phase incoherent superconductivity [11] from the signatures of nontrivial charge ordering [13], it is imperative to examine their evolution with doping and magnetic field using techniques sensitive to both phenomena [14]. The large resistivity anisotropy in LBCO ($\rho_c/\rho_{ab} \sim 10^3$, [17]) severely limits attempts to detect their presence using the anomalous Hall effect—due to unavoidable artifacts resulting from the c-axis pickup [24]. In contrast, the near-isotropic thermoelectric properties of LBCO [27] enable the field-symmetric Nernst coefficient, $e_N^S(T)$, to probe their signatures with the requisite sensitivity. Having determined the characteristic temperature scales of stripe and superconducting phases for our samples, we thus turn to the Nernst effect measurements forming the nucleus of this work.

The Nernst coefficient, $e_N = V_y/\nabla T_x$, corresponds to the transverse voltage V_y generated due to a longitudinal thermal gradient ∇T_x. It is typically observed at a finite magnetic field, and in the cuprates, it has been attributed to moving vortices [28,29], Gaussian fluctuations [30], or to quasiparticles arising from fluctuating stripes [31,32]. While the aforementioned *field antisymmetric*, or conventional Nernst coefficient is determined entirely from transverse thermoelectric measurements at fields $\pm H$ [$e_N^A = (S_{xy}(H) - S_{xy}(-H))/2$], this is not possible for the *field-symmetric*, unconventional component of interest to us [$e_N^s = (S_{xy}(H) + S_{xy}(-H))/2$]. For example, at zero field, the observed signal (S_{xy}) unavoidably contains a longitudinal S_{xx} pickup due to a slight misalignment of the contact leads [Fig. 2(b)]. Therefore we obtain the true zero-field Nernst (ZFN) coefficient $e_N^0(T)$ [and, by extension, $e_N^s(T)$ at finite fields] by removing the S_{xx} contribution to S_{xy}, i.e., $e_N^0(T) = S_{xy}(T) - S_{xx}(T)/k$ [11], where $S_{xx}(T)$ and

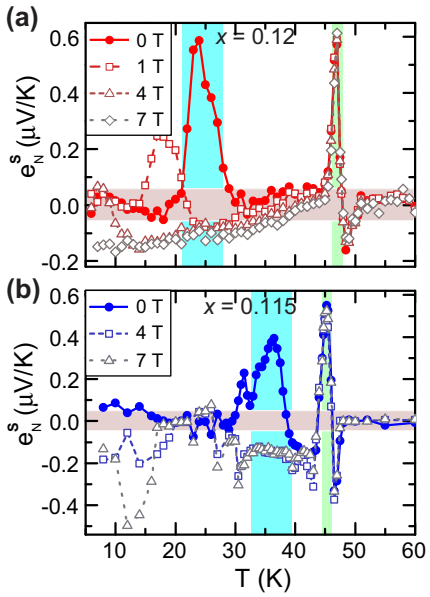

FIG. 3. Field dependence of symmetric Nernst effect. The field-symmetric part of the Nernst coefficient, $e_N^S(T)$ at various magnetic fields for (a) $x = 0.12$ and (b) $x = 0.115$. The sharp $\sim T_{CO}$ feature is field-invariant, while the lower-temperature feature is strongly suppressed by magnetic field.

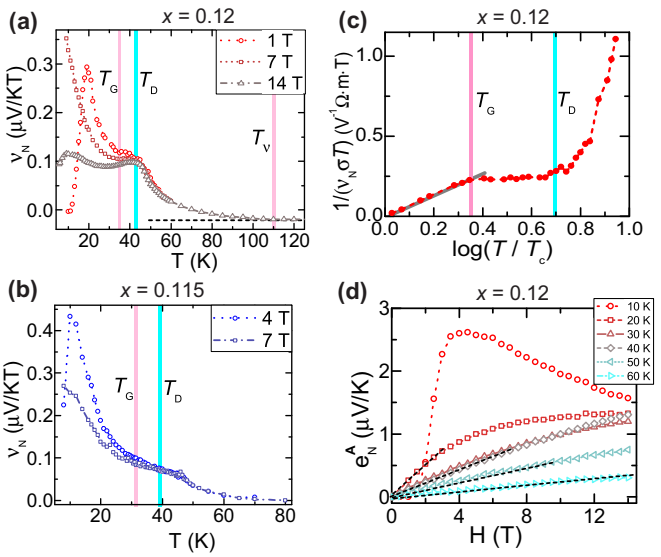

FIG. 4. Conventional Nernst effect. (a) and (b) Temperature dependence of the normalized antisymmetric Nernst coefficient, $\nu_N(T) = e_N^A(T)/H$, at various magnetic fields for (a) $x = 0.12$, and (b) $x = 0.115$. Shaded lines indicate a deviation from the constant background ($T_\nu \sim 110$ K), and characteristic features at T_D and T_G. (c) Plot of $1/(\nu_N \sigma T)$ vs $\ln(T/T_c)$ for $x = 0.12$, with the solid gray line indicating a linear fit to Gaussian fluctuation theory [35,36] below $T_G = 33$ K. (d) Magnetic field dependence of the antisymmetric Nernst coefficient $e_N^A(H)$ at various temperatures for $x = 0.12$, showing the onset of nonlinearity below T_D.

$S_{xy}(T)$ are measured simultaneously [schematic in Fig. 2(a), details in Ref. [24]).

The ZFN coefficient $e_N^0(T)$ measured as a function of temperature using this compensated technique for $x = 0.12$ and 0.115 [see Figs. 2(c) and 2(d), respectively] shows several features at characteristic transition temperatures that are consistent across doping. First, $e_N^0(T)$ is finite only for $T_{c,R} < T \lesssim T_{CO}$, i.e., in the presence of static stripes, yet in the absence of bulk superconductivity, as reported for $x = 0.125$ [11]. Second, $e_N^0(T)$ can be bipolar [Fig. 2(d)] in contrast with [11], and the exact behavior is reproduced through multiple temperature cycles. Third, we observe a broad hump (of width ~ 8 K) just above $T_{c,R}$, which can be ascribed to spontaneous vortex generation [11]. Fourth, and crucially, we observe a *sharp peak* (of width ~ 1 K) at a temperature previously identified as T_{CO}. This T_{CO} peak, also visible in the raw data [Fig. 2(b)] has been hitherto unobserved, likely due to its sharp linewidth; our high-temperature resolution ($\sim$0.25 K) and small-temperature gradients ($\sim$0.1 K/mm) enable its detection. We reiterate that such a sharp peak is in contrast to a broad hump expected from the presence of vortices [11]. Importantly, its coincidence with the onset of stripe charge order (T_{CO}) is suggestive of its origin.

Having identified features of interest in the ZFN data, we now turn to the field-symmetric evolution of these data (e_N^S, shown in Fig. 3) to further understand the origin of these features. The two peaked features identified previously have a remarkably contrasting field dependent behavior—consistent across doping. First, the broad hump just above $T_{c,R}$ is strongly suppressed with the field—it is much reduced in magnitude and is observed at lower temperatures. This is consistent with its expected origin from the spontaneous generation of vortices of one sign, which would be stabilized by TRSB [11].

In contrast, the sharp peak at T_{CO} has no observable field dependence in position or magnitude, maintaining a robust presence at T_{CO} across field and doping. This strongly suggests that the latter peak does not have a superconducting origin, and could instead emerge from other nontrivial symmetry breaking phenomena [13]. Finally, we also note the field dependence of the $e_N^S(T)$ background emerging at or just below T_{CO}, and persisting to lower temperatures.

The conventional Nernst effect has been extensively utilized to probe superconducting and quasiparticle fluctuations in the cuprates [28,31]. Figures 4(a) and 4(b) show the temperature dependence of the field-normalized, antisymmetric Nernst coefficient of LBCO-0.120, $\nu_N(T) = e_N^A(T)/H$, measured at various magnetic fields for the two doping values. At high temperatures, the near-constant ν_N results from quasiparticle transport [28]. Below the Nernst onset temperature $T_\nu \sim 110$ K, $\nu_N(T)$ deviates from the background, with a kink observed at T_{CO}. The suppression of ν_N by a magnetic field at temperatures below the onset of diamagnetism, T_D, is a clear signature of superconducting vortices [28,30,33,34]. This may result from either vortex excitations produced by phase fluctuations [28,33] or from Gaussian amplitude fluctuations caused by short-lived Cooper pairs [30,34]. In our case, ν_N increases dramatically below $T_G = 33$ K for $x = 0.12$—the onset temperature of Gaussian fluctuations. This is verified in Fig. 4(c), wherein a linear relationship is observed between $1/(\nu_N \sigma T)$ and $\ln(T/T_c)$ below T_G—indicating the dominance of Gaussian fluctuations [30,35,36] for $T_c < T < T_G$. Meanwhile, the superconducting signatures observed over

$T_G < T < T_D$ are likely due to vortex excitations. Finally, the absence of any measurable field-dependence signatures in v_N at T_{CO} corroborate the nonsuperconducting origin of the T_{CO} peak in the complementary ZFN measurements.

III. DISCUSSION

Our doping and field-dependent studies show that the symmetric Nernst effect signal observed in near-1/8 LBCO is comprised of two distinct components—a broad, field-dependent hump above $T_{c,R}$ of superconducting origin, and a sharp field-independent peak at T_{CO}. The observed behavior of the broad hump with doping and field substantiates prior reports at $x = 1/8$ of spontaneously generated vortices arising from TRSB [11]. In contrast, the hitherto unobserved robust peak at T_{CO}, unchanged with field, is suggestive of a stripe charge order origin. It is worth emphasizing that the observed result is a large, spontaneously generated *transverse electric field* at T_{CO} in response to a longitudinal thermal gradient. Having ruled out a superconducting origin, we consider the possibility that this results from the heat current going off-axis for extrinsic reasons, either induced by the contacts, or sample inhomogeneity. First, we point out that repeated (3–5 times) measurements across multiple samples for each doping with fresh electrical and thermal contacts show a T_{CO} peak constant in magnitude within measurement error—discounting contact-related artifacts. Next, the possibility of marked physical or chemical inhomogeneity deeper inside the sample causing this effect can also be ruled out as these should be detectable within the complementary $\rho_{xx}(T)$, $\rho_{xy}(T)$, $S_{xx}(T)$, and $M(T)$ measurements, which are instead consistent with the expected behavior at the corresponding doping [24]. Finally, in a perfectly crystalline sample, it is also possible that the onset of an orthorhombic to tetragonal structural transition, or the emergence of unidirectional charge stripes could drastically alter the thermal transport properties, introducing a transverse component to the thermal current. Here, it is worth noting that our samples are not detwinned, and such unidirectional behavior is expected to average out over the sample size, as evidenced in Hall measurements [24]. Moreover, our measurements of transverse thermal gradients across this temperature range show that any such transverse effects would be at least five times smaller than the the observed sharp, sizable feature at T_{CO} [24]. Furthermore, since the sample is heated to high temperatures ($\sim$ 700 K, for contact preparation) between successive measurements, the presence of a quantitatively reproducible peak is not tenable in such a scenario.

Finally, we examine plausible scenarios wherein the T_{CO} peak emerges from intrinsic effects resulting from the onset of stripe charge order in the LTT phase. One possibility is that the presence of some tetragonal symmetry breaking could result in the mixing of longitudinal and transverse transport coefficients. While such effects would be small or absent in a perfectly tetragonal crystal, they could be induced by charge or superconducting stripes, and would be preferentially oriented along crystallographic directions. Another possibility is that this peak results from the point-group symmetry breaking emerging from nontrivial stacking of stripes [14,22], as observed in Kerr effect measurements of similar samples [12]. In this latter case, one would expect PSB, and thus the ZFN signal to persist to well below T_{CO}. While the peaklike manifestation of the ZFN signal could, in principle, result from the interplay of a PSB signal and the field-dependent background, a quantitative explanation of the observations is imperative.

In summary, we have performed a detailed field-dependent investigation of the thermoelectric coefficients of near-1/8 LBCO at multiple dopings. Our symmetric Nernst effect signal is comprised of two distinct components—a broad, field-dependent hump above $T_{c,R}$ of superconducting origin, and a sharp field-independent peak at T_{CO}. While the former is consistent with prior reports indicative of spontaneous TRSB, the latter, likely of stripe charge order origin, merits a comprehensive theoretical explanation.

ACKNOWLEDGMENTS

We are grateful to Ivar Martin for insightful discussions. A.S. and X.Y.T. contributed equally to this work. The work was supported by the National Research Foundation, Singapore, through Grant NRF-CRP4-2008-04. The work at AIST was supported by JSPS Grants-in-Aid for Scientific Research (Grant No. 22560018).

[1] M. R. Norman, Science **332**, 196 (2011).
[2] P. A. Lee, Phys. Rev. X **4**, 031017 (2014).
[3] L. Taillefer, J. Phys.: Condens. Matter **21**, 164212 (2009).
[4] S. E. Sebastian, N. Harrison, C. H. Mielke, R. Liang, D. A. Bonn, W. N. Hardy, and G. G. Lonzarich, Phys. Rev. Lett. **103**, 256405 (2009).
[5] W. D. Wise, M. C. Boyer, K. Chatterjee, T. Kondo, T. Takeuchi, H. Ikuta, Y. Wang, and E. W. Hudson, Nat. Phys. **4**, 696 (2008).
[6] V. J. Emery, S. A. Kivelson, and J. M. Tranquada, Proc. Natl. Acad. Sci. USA **96**, 8814 (1999).
[7] R.-H. He, M. Hashimoto, H. Karapetyan, J. D. Koralek, J. P. Hinton, J. P. Testaud, V. Nathan, Y. Yoshida, H. Yao, K. Tanaka, W. Meevasana, R. G. Moore, D. H. Lu, S.-K. Mo, M. Ishikado, H. Eisaki, Z. Hussain, T. P. Devereaux, S. A. Kivelson, J. Orenstein, A. Kapitulnik, and Z.-X. Shen, Science **331**, 1579 (2011).
[8] J. Xia, E. Schemm, G. Deutscher, S. A. Kivelson, D. A. Bonn, W. N. Hardy, R. Liang, W. Siemons, G. Koster, M. M. Fejer, and A. Kapitulnik, Phys. Rev. Lett. **100**, 127002 (2008).
[9] M. Fujita, H. Goka, K. Yamada, J. M. Tranquada, and L. P. Regnault, Phys. Rev. B **70**, 104517 (2004).
[10] M. Hücker, M. v. Zimmermann, G. D. Gu, Z. J. Xu, J. S. Wen, G. Xu, H. J. Kang, A. Zheludev, and J. M. Tranquada, Phys. Rev. B **83**, 104506 (2011).
[11] L. Li, N. Alidoust, J. M. Tranquada, G. D. Gu, and N. P. Ong, Phys. Rev. Lett. **107**, 277001 (2011).

[12] H. Karapetyan, M. Hücker, G. D. Gu, J. M. Tranquada, M. Fejer, J. Xia, and A. Kapitulnik, Phys. Rev. Lett. **109**, 147001 (2012).
[13] H. Karapetyan, J. Xia, M. Hücker, G. D. Gu, J. M. Tranquada, M. M. Fejer, and A. Kapitulnik, Phys. Rev. Lett. **112**, 047003 (2014).
[14] P. Hosur, A. Kapitulnik, S. A. Kivelson, J. Orenstein, and S. Raghu, Phys. Rev. B **87**, 115116 (2013).
[15] T. Valla, A. V. Fedorov, J. Lee, J. C. Davis, and G. D. Gu, Science **314**, 1914 (2006).
[16] R.-H. He, K. Tanaka, S.-K. Mo, T. Sasagawa, M. Fujita, T. Adachi, N. Mannella, K. Yamada, Y. Koike, Z. Hussain, and Z.-X. Shen, Nat. Phys. **5**, 119 (2008).
[17] Q. Li, M. Hücker, G. D. Gu, A. M. Tsvelik, and J. M. Tranquada, Phys. Rev. Lett. **99**, 067001 (2007).
[18] J. M. Tranquada, G. D. Gu, M. Hücker, Q. Jie, H.-J. Kang, R. Klingeler, Q. Li, N. Tristan, J. S. Wen, G. Xu, Z. A. Xu, J. Zhou, and M. von Zimmermann, Phys. Rev. B **78**, 174529 (2008).
[19] J. Orenstein and J. E. Moore, Phys. Rev. B **87**, 165110 (2013).
[20] S. Chakravarty, Phys. Rev. B **89**, 087101 (2014).
[21] N. P. Armitage, Phys. Rev. B **90**, 035135 (2014).
[22] P. Hosur, A. Kapitulnik, S. A. Kivelson, J. Orenstein, S. Raghu, W. Cho, and A. Fried, Phys. Rev. B **91**, 039908(E) (2015).
[23] T. Ito, T. Ushiyama, Y. Yanagisawa, Y. Tomioka, I. Shindo, and A. Yanase, J. Cryst. Growth **363**, 264 (2013).
[24] See Supplemental Material at http://link.aps.org/supplemental/10.1103/PhysRevB.93.054512 for details on sample preparation, measurement techniques, supporting magnetotransport measurements, and consistency checks for thermoelectric measurements.
[25] M. Hücker, G. D. Gu, and J. M. Tranquada, Phys. Rev. B **78**, 214507 (2008).
[26] M. Hücker, M. V. Zimmermann, M. Debessai, J. S. Schilling, J. M. Tranquada, and G. D. Gu, Phys. Rev. Lett. **104**, 057004 (2010).
[27] Y. Nakamura and S. Uchida, Phys. Rev. B **47**, 8369 (1993).
[28] Y. Wang, L. Li, and N. P. Ong, Phys. Rev. B **73**, 024510 (2006).
[29] L. Li, J. G. Checkelsky, S. Komiya, Y. Ando, and N. P. Ong, Nat. Phys. **3**, 311 (2007).
[30] I. Ussishkin, S. L.Sondhi, and D. A. Huse, Phys. Rev. Lett. **89**, 287001 (2002).
[31] O. Cyr-Choinière, R. Daou, F. Laliberté, D. LeBoeuf, N. Doiron-Leyraud, J. Chang, J.-Q. Yan, J.-G. Cheng, J.-S. Zhou, J. B. Goodenough, S. Pyon, T. Takayama, H. Takagi, Y. Tanaka, and L. Taillefer, Nature (London) **458**, 743 (2009).
[32] J. Chang, R. Daou, C. Proust, D. LeBoeuf, N. Doiron-Leyraud, F. Laliberté, B. Pingault, B. J. Ramshaw, R. Liang, D. A. Bonn, W. N. Hardy, H. Takagi, A. B. Antunes, I. Sheikin, K. Behnia, and L. Taillefer, Phys. Rev. Lett. **104**, 057005 (2010).
[33] Z. A. Xu, N. P. Ong, Y. Wang, T. Kakeshita, and S. Uchida, Nature (London) **406**, 486 (2000).
[34] I. Kokanović, J. R. Cooper, and M. Matusiak, Phys. Rev. Lett. **102**, 187002 (2009).
[35] M. N. Serbyn, M. A. Skvortsov, A. A. Varlamov, and V. Galitski, Phys. Rev. Lett. **102**, 067001 (2009).
[36] K. Michaeli and A. M. Finkel'stein, Europhys. Lett. **86**, 27007 (2009).